



Synthesis of hollow Mo₂C/carbon spheres, and their application to simultaneous electrochemical detection of hydroquinone, catechol, and resorcinol

Hailong Ren¹ · Yang Zhang² · Longlong Liu¹ · Yangguang Li¹ · Dongyang Wang¹ · Ruyue Zhang³ · Wenjing Zhang¹ · Yingchun Li^{2,3} · Bang-Ce Ye^{1,4}

Received: 19 December 2018 / Accepted: 10 April 2019 / Published online: 27 April 2019
© Springer-Verlag GmbH Austria, part of Springer Nature 2019

Abstract

Hollow molybdenum-dopamine spheres were synthesized and thermally annealed to form hollow Mo₂C/C spheres. The morphology, composition and electrochemical behavior of spheres were characterized. A glassy carbon electrode (GCE) was modified with the spheres and then used for simultaneous detection of hydroquinone (HQ), catechol (CC), and resorcinol (RS). Distinct oxidation peaks can be observed for HQ, CC and RS at potentials of -0.004 V, 0.10 V and 0.44 V (vs. SCE). The responses to HQ, CC and RS are linear in the concentration ranges of 0.3~1000 μM, 2~2000 μM and 3~600 μM, respectively. The corresponding detection limits are 0.12, 0.19 and 1.1 μM (at S/N=3). The sensor was then applied to quantify HQ, CC, and RS in tap water, river water and vegetable juice. Recoveries ranged from 93.5% to 106.5%. The modified GCE is repeatable, reproducible, stable and selective for HQ, CC and RS.

Keywords Hollow Mo₂C/C · Isomeric dihydroxybenzene · Scanning electron microscopy · Cyclic voltammetry · Differential pulse voltammetry · Simultaneous determination · Electrochemical detection · Water analysis

Hailong Ren and Yang Zhang contributed equally to this work.

Electronic supplementary material The online version of this article (<https://doi.org/10.1007/s00604-019-3432-7>) contains supplementary material, which is available to authorized users.

✉ Yingchun Li
liyinchun@hit.edu.cn

✉ Bang-Ce Ye
bcye@ecust.edu.cn

¹ Key Laboratory for Green Processing of Chemical Engineering of Xinjiang Bingtuan, School of Chemistry and Chemical Engineering, Shihezi University, Shihezi 832003, China

² College of Science, Harbin Institute of Technology, Shenzhen 518055, China

³ Key Laboratory of Xinjiang Phytomedicine Resources for Ministry of Education, School of Pharmacy, Shihezi University, Shihezi 832000, China

⁴ State Key Laboratory of Bioreactor Engineering, East China University of Science and Technology, Shanghai 200237, China

Introduction

Hydroquinone (HQ), catechol (CC) and resorcinol (RS) are commonly used as intermediates in industry and agriculture. Due to their high toxicities and low degradabilities, the dihydroxybenzene isomers were categorized as environmental pollutants [1]. Electrochemical methods have attracted more and more attention because of their unique advantages, such as fast response, low cost, simple operation and excellent sensitivity [2]. Since HQ, CC and RS are electrochemically active substances, they can be measured by electrochemical method. However, their redox peak potentials tend to overlap, which cannot be separated by unmodified electrode like bare glassy carbon electrode (GCE). Thus, developing electrode modification materials for appropriately catalyzing the electrochemical reactions of the three dihydroxybenzene isomers is necessary for their simultaneous detection.

Some electrochemical methods based on carbon nanomaterials have been reported for detection of dihydroxybenzene isomers. For example, Huang et al. used porous carbon material doped with an iron species modified GCE to achieve simultaneous detection of hydroquinone and catechol [3]. Li's group reported that cerium phosphate nanotubes had good electrochemical catalytic activity for dihydroxybenzene isomers [4]. Lorena Athie Goulart used synergic effect of silver nanoparticles and carbon nanotubes voltammetric simultaneous determination of hydroquinone, catechol, bisphenol A and phenol [5]. Rajkumar et al. reported voltammetric determination of catechol and hydroquinone using nitrogen-doped multiwalled carbon nanotubes modified with nickel nanoparticles [6]. Naghian et al. synthesized SnO₂/CuS, SnO₂/SnS and Cu@SnO₂/SnS nanocomposites and used it to modify carbon paste electrodes for detection of paracetamol and hydroquinone [7]. However, these sensors have some disadvantages such as time-consuming synthesis, laborious procedure, high cost, poor reproducibility and narrow detection range, which hinder their further application. Therefore, it is still of great significance to find reliable material modified electrodes to enhance electrochemical signals, reduce background current and achieve simultaneous detection.

It is well known that molybdenum-based materials have decent features like low cost, high catalytic performance and chemical stability [8–10]. The reported Mo-involved materials used in electrochemical fields include molybdenum dioxide (MoO₂) [11, 12], molybdenum disulfide (MoS₂) [13, 14], molybdenum carbide (Mo₂C) [12, 14, 15], etc., which own good electrical conductivity and catalytic property as well. Moreover, studies have showed that hollow nanomaterials exhibited improved performance due to the increased surface area [16]. A few Mo-based hollow nanocomposites have been reported, such as hollow microspheres [17, 18] and tripleshelled hollow spheres [19, 20]. There are also some molybdenum-based materials for electrochemical sensing, such as: Li et al. used molybdenum disulfide nanosheets supported Au-Pd bimetallic nanoparticles for non-enzymatic electrochemical sensing of hydrogen peroxide and glucose [21]. Rajkumar et al. reported voltammetric determination of bisphenol A using molybdenum disulfide/Au nanorod composites modified glassy carbon electrode [22].

Hollow molybdenum-dopamine spheres (HMPDSs) were synthesized easily by one-step method at room temperature. The HMPDSs were annealed at 900 °C for 5 h under Ar to obtain hollow Mo₂C/C spheres (HMCCSs). The Brunauer-Emmett-Teller (BET) experiment and electrochemical characterization confirmed that HMCCSs have large surface area and high electrical conductivity. The electrochemical behaviors of dihydroxybenzene isomers at HMCCSs/GCE were studied by cyclic voltammetry (CV) and differential pulse voltammetry (DPV). HMCCSs/GCE was used for

simultaneous assay of HQ, CC and RS, showing wide linear range, good stability, high sensitivity and reproductivity. In addition, HMCCSs modified GCE has been successfully applied to the detection of HQ, CC and RS in real samples.

Experimental section

Reagents and instruments

Hydroquinone (HQ), catechol (CC), resorcinol (RC), ammonium molybdate tetrahydrate ((NH₄)₆Mo₇O₂₄·4H₂O) and dopamine hydrochloride were purchased from Aladdin Co. Ltd. (Shanghai, China; www.aladdin-e.com). N, N-dimethyl formamide (DMF) was purchased from Sigma-Aldrich (Shanghai, China; www.sigmaaldrich.com). Other reagents and chemicals, such as K₃[Fe(CN)₆], K₄[Fe(CN)₆], KNO₃, KCl, HCl, NaOH and ethanol were purchased from Titan Scientific Co. Ltd. (Shanghai, China; www.tansoole.com). Phosphate buffer (PB, 0.1 mol L⁻¹) was prepared by mixing solution of 0.1 mol L⁻¹ KH₂PO₄ and 0.1 mol L⁻¹ K₂HPO₄, and the pH was adjusted with HCl or NaOH. All solutions were prepared using ultrapure water. All chemicals were analytical level and used without further purification.

All electrochemical experiments were performed on a CHI660E electrochemical workstation (Chenhua Instruments Co, Shanghai, China; www.chinstr.com) including cyclic voltammetry (CV), electrochemical impedance spectroscopy (EIS) and differential pulse voltammetry (DPV). A classical three-electrode system include a bare or modified glassy carbon electrode (GCE, 3 mm diameter), a saturated calomel electrode (SCE) and a platinum wire (0.5 mm in diameter and 34 mm in length) as the working, reference and auxiliary electrode, respectively. The surface topography was observed with scanning electron microscopy (SEM, Zeiss Supra55VP, Germany; www.bruker.com). Fourier transform infrared (FTIR) spectroscopy was performed on a Nicolet iS50 spectrometer (USA). The composition of the material was characterized by energy dispersive X-ray spectroscopy (EDS, Bruker XFlash 5010, Germany; www.bruker.com). The specific surface area of Mo₂C/C was measured with a Brunauer-Emmett-Teller (BET, Quantachrome NOVA 1000) experiment. The size and morphology of HMCCSs was observed with a transmission electron microscopy (TEM, JEM-1200EX) at 120 kV. Material structure was characterized by X-ray powder diffraction (XRD) on a Bruker D8 advance X-ray diffractometer (Cu-Kα, λ = 1.5418 Å, Bruker XFlash-SDD-5010, Germany; www.bruker.com) from 10° to 90°. HPLC was performed with a Shimadzu system comprising of LC-10A pumps and an SPD-10A UV-detector (Japan; www.shimadzu.com.cn). X-ray photoelectron spectroscopy (XPS) was performed using an Al 18 Kα X-ray source

(Escalab 250, Thermo Fisher Scientific, USA; www.thermofisher.com).

Fabrication of the HMCCS/GCE

HMCCSs/GCE was prepared by simple drop-coating. Bare glassy carbon electrode (GCE) was polished with 0.3 μm and 0.05 μm alumina power slurries, followed by successive washing with ethanol and distilled water, and dried at room temperature. HMCCSs was evenly dispersed in DMF (1 mg mL^{-1}) by ultrasonication for 40 min and 5 μL of the HMCCSs suspension was dropped onto surface of the working electrode and dried under infrared lamp. The preparation procedure of HMCCSs/GCE is illustrated in Scheme 1.

Electrochemical measurement

Detection of HQ, CC and RS was performed in 0.1 M PB (pH 7.0) at room temperature. Firstly, standard stock solutions of different concentrations of HQ, CC and RS were prepared by dissolving HQ, CC and RS in 0.1 M PB (pH 7.0). Subsequently, the three-electrode system was placed in a 25 mL 0.1 M PB (pH 7.0) cell and peak currents intensity of HQ, CC and RS on different electrodes were recorded by cyclic voltammetry (CV) and differential pulse voltammetry (DPV). CV and DPV were carried out in the potential range

from -0.2 V to $+0.8 \text{ V}$. Electrochemical impedance spectroscopy was performed in solution containing 5 mM $[\text{Fe}(\text{CN})_6]^{3-/4-}$ and 0.1 M KCl in the frequency range from 0.01 Hz to 100 kHz.

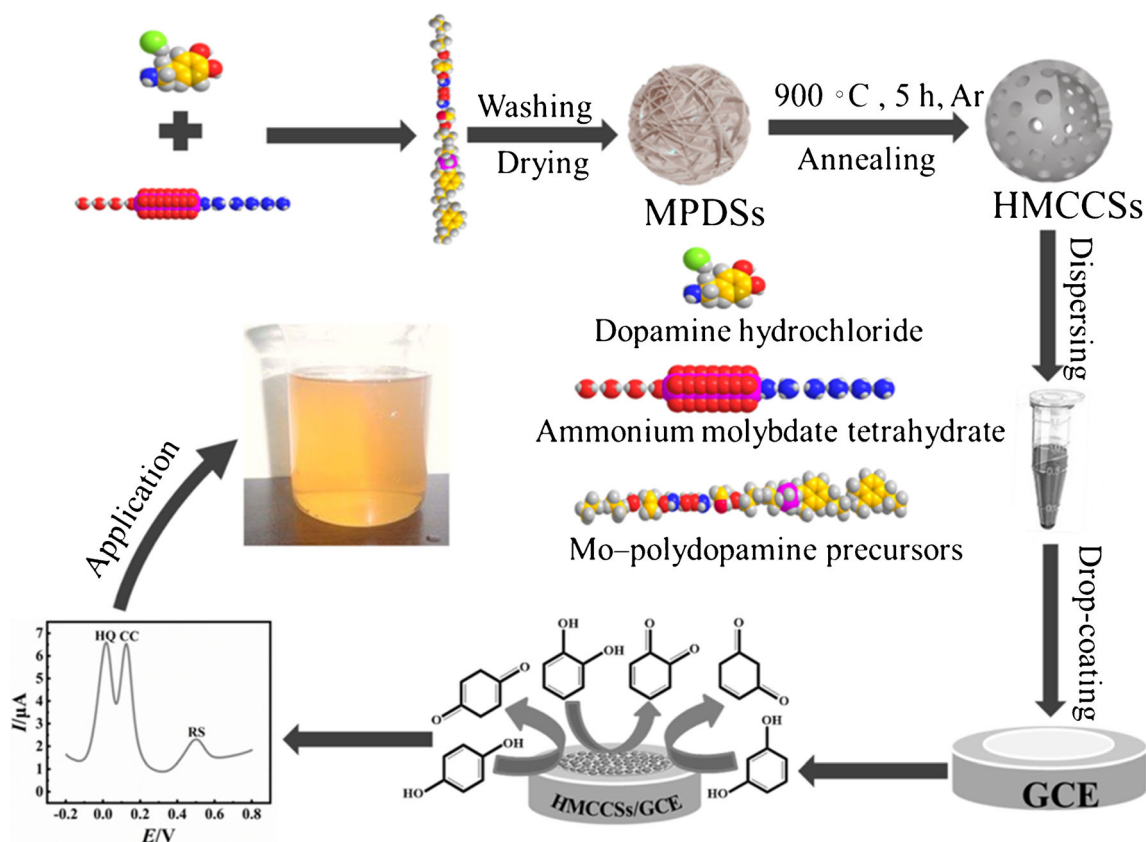
Detection of HQ, CC and RS in real samples

In order to evaluate the practical applicability of the prepared sensor, tap water, river water and vegetable juice samples were assayed via spiked recovery experiment. Fresh vegetables (spinach and romaine) were ground into juice, and centrifuged at 5000 rpm for 10 min, and the supernatant was collected. The supernatant was diluted 20 times with 0.1 M PB (pH 7.0) before measurement in order to reduce the matrix effect. Afterwards, standard solution with analyte at different concentrations was added into the vegetable juice or water samples at volumetric ratio of 2: 1. Then the spike real samples were tested.

Results and discussion

Choice of materials

It is well known that sensing materials are critical to sensitivity and selectivity of the sensor. Among the materials adopted,



Scheme 1 The schematic representation of HMCCSs/GCE preparation.

nano-scale porous carbon is a class of widely used one due to its porous structure, large specific surface area, low cost and high stability. However, in the previously published reports, strong oxidants (sulfuric acid, potassium permanganate, nitric acid, etc.) are often employed in synthesizing carbon nanomaterials, which may cause some harm to operators. In contrast, the synthesis conditions in our paper are facile and mild (ethanol and water as solvents), and the precursor reaction occurs at room temperature. Introduction of metal nanoparticles is an effective way in boosting sensing performance, and compared with the noble metals like Au, Pt, etc., Mo is more cost-efficient.

Morphologic and structural characterization of hollow molybdenum-dopamine spheres (HMPDSs) and of hollow Mo₂C/C spheres (HMCCSs)

The surface morphology of HMPDSs and HMCCSs were investigated by SEM and TEM. As shown in Fig. 1a, HMPDSs are uniform spheres consisting of a layered Mo – dopamine complex with a diameter of about 600 nm. After annealing, HMCCSs

retain the original morphology and structure of HMPDSs without any aggregation and their diameter is around 500 nm (Fig. 1b). After annealing, due to partial thermal decomposition of organic ligands, some organic framework collapsed and some small pores are formed, which might cause decrease in particle size and increase in surface area. TEM image of HMPDSs further confirms that HMPDSs own hollow core nanostructure with many lamellas (Fig. 1c). As shown in Fig. 1d, it can be observed that HMCCSs also has hollow and porous structure. Dark particles may be the result of aggregation of Mo₂C nanoparticles. It can also be seen from the EDS mapping that the main element in the dark particles is Mo. The energy dispersive X-ray spectroscopy (EDS) maps in Fig. 1e confirm the porous structure of HMCCSs, in which C, N and Mo elements are evenly distributed. The Brunauer-Emmett-Teller (BET) specific surface area of HMPDSs and HMCCSs was measured by nitrogen adsorption-desorption curve, and the area is 224 m² g⁻¹ and 588 m² g⁻¹, respectively (Fig. S1A and S1C). Besides, the average pore size of HMPDSs and HMCCSs ranges from 10 nm to 138 nm and 10 nm to 128 nm, respectively (Fig. S1B and S1D).

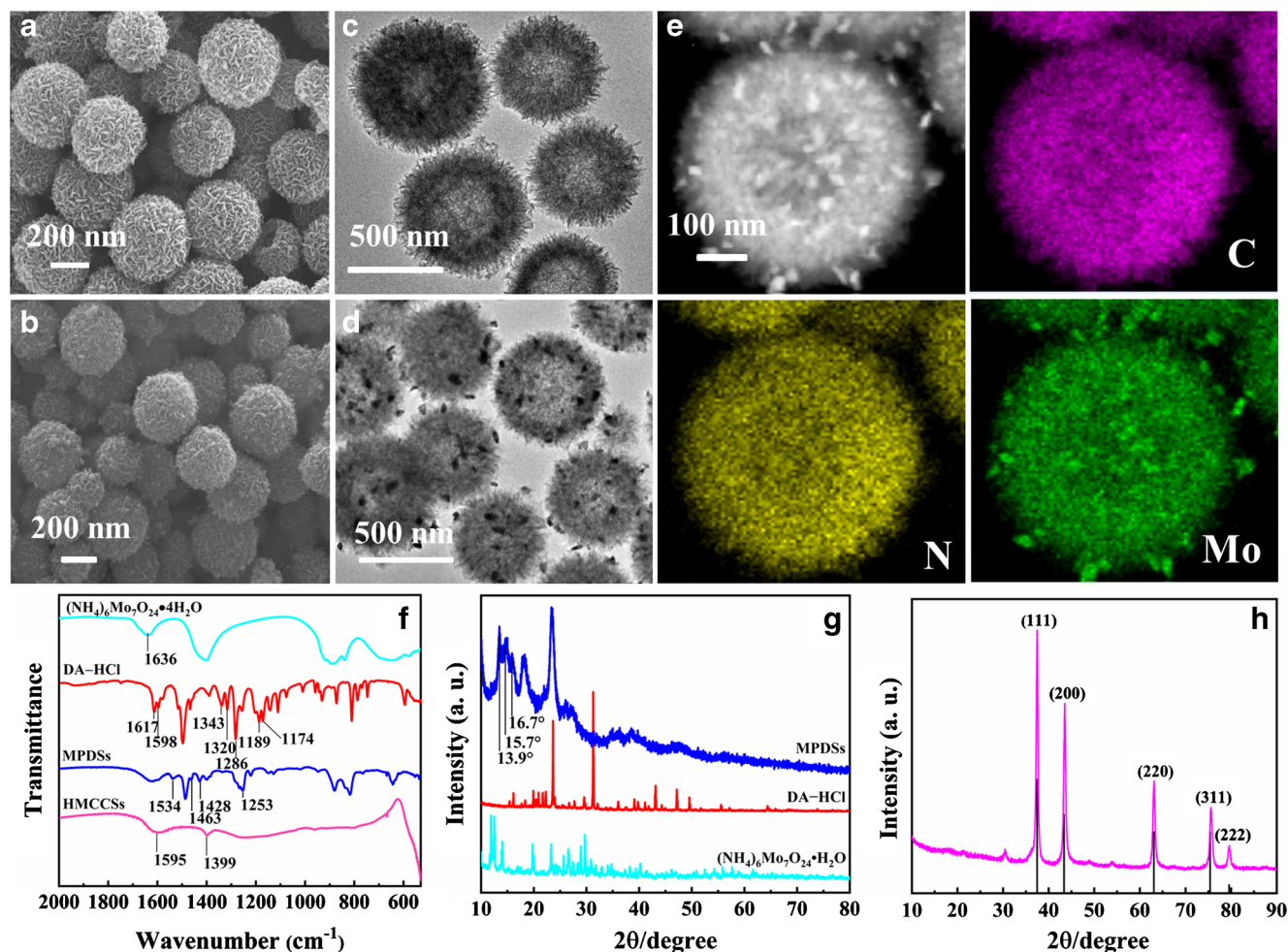


Fig. 1 SEM images of **a** hollow molybdenum-dopamine spheres (HMPDSs), **b** hollow Mo₂C/C spheres (HMCCSs), TEM image of **c** HMPDSs, **d** HMCCSs, **e** EDS mapping of HMCCSs, **f** FTIR spectra of

(NH₄)₆Mo₇O₂₄•4H₂O, DA – HCl, HMPDSs, and HMCCSs. XRD patterns of **g** HMPDSs, DA–HCl, (NH₄)₆Mo₇O₂₄•4H₂O, and **h** HMCCSs

The bonds of $(\text{NH}_4)_6\text{Mo}_7\text{O}_{24}\cdot 4\text{H}_2\text{O}$, dopamine–HCl (DA–HCl), HMPDSs, and HMCCSs were studied by Fourier transform infrared spectroscopy (FTIR) (Fig. 1f). The peaks of $(\text{NH}_4)_6\text{Mo}_7\text{O}_{24}\cdot 4\text{H}_2\text{O}$ at 1636 cm^{-1} corresponded to the bending vibrations of N–H. The strong absorption bands at 1617 cm^{-1} and 1598 cm^{-1} were assigned to the bending vibration of the primary amine N–H bond in DA–HCl. The absorption bands at 1343 cm^{-1} , 1320 cm^{-1} and 1286 cm^{-1} are attributed to the bending vibration of O–H and the stretching vibration of C–O on aromatic rings. After chelation, the bands of HMPDSs in the vicinity of 1619, 1598, 1343 and 1320 cm^{-1} are significantly reduced, and some new peaks are observed at 1534, 1463, 1428 and 1253 cm^{-1} . These are attributed to the bending vibration of the C–N–C, C–C=N and indicates the formation of indole structure. The peaks of HMCCSs at 1595 cm^{-1} and 1399 cm^{-1} are ascribable to stretching vibration of C=C, bending vibration of N–H and C–N, demonstrating that the indole structure still exists after annealing.

The XRD patterns of HMPDSs, DA–HCl, and $(\text{NH}_4)_6\text{Mo}_7\text{O}_{24}\cdot 4\text{H}_2\text{O}$ is shown in Fig. 1g. Compared with dopamine–HCl (DA–HCl) and ammonium molybdate tetrahydrate, HMPDSs show several strong peaks at $2\theta = 13.9^\circ$, 15.7° and 16.7° , indicating that a new phase is formed with interaction between MoO_4^{2-} and hydroxyl groups of DA–HCl. The diffraction peaks of HMCCSs appear at 37.76° , 43.69° , 63.39° , 75.72° , and 79.86° corresponding to the (111) (200) (220) (311) (222) plane, respectively, which are basically consistent with the JCPDS card (PDF#15–0457) (Fig. 1h). The results show that the HMCCSs were successfully synthesized.

The elemental composition and chemical state of the HMCCSs were determined by X-ray electron spectroscopy (XPS). Fig. S2A investigates the different peaks at 231.08 (Mo 3d), 283.08.5 (C 1s), 397.08 (N 1s), 415 (Mo 3p) and 529.08 eV (O 1s) [23]. In Fig. S2B, the two peaks at 227.18 and 230.48 eV can be designated as Mo $3d_{5/2}$ and Mo $3d_{3/2}$ of Mo^{2+} , which is consistent with the carbide. The binding energies at 231.08 and 234.28 eV can be assigned to Mo $3d_{5/2}$ and Mo $3d_{3/2}$ of Mo^{6+} . The binding energy of Mo^{4+} is 228.08 eV, which is derived from MoO_2 , Mo^{6+} and Mo^{4+} when the surface of Mo_2C is oxidized in contact with air [24].

Electrochemical characterization of HMCCSs/GCE

The electrochemical properties of GCE, HMPDSs/GCE and HMCCSs/GCE were characterized by electrochemical impedance spectroscopy (EIS) and cyclic voltammetry (CV) in 5 mM $[\text{Fe}(\text{CN})_6]^{3-/4-}$ redox probe solution. As shown in Fig. 2a, the increase order of oxidation and reduction peak currents value of the modified electrode is $I_{\text{HMCCSs/GCE}} > I_{\text{HMPDSs/GCE}} > I_{\text{GCE}}$. The results demonstrated that HMPDSs and HMCCSs can effectively

improve electrical conductivity and increase electron transport rate on the electrode surface. The peak current of HMCCSs/GCE is higher than HMPDSs/GCE, which can be attributed to the formation of a porous structure after carbonization of MPDS providing more active sites for electron transport. The results indicate that the porous structure of HMCCSs and catalytic effect of Mo improve the conductivity and promote electron transfer at the modified electrodes.

Electrochemical impedance spectroscopy (EIS) consists of a straight lines part in the low frequency regions and a semi-circular part in the high frequency regions, indicating that the diffusion process and the electron transfer process occurred at the electrode (Fig. 2b). The inset of Fig. 2b is an electrical equivalent cycle fit impedance plot. The charge transfer resistance (R_{ct}) was estimated through calculating the semicircle diameter. According to the results shown in Fig. 2b, R_{ct} of bare GCE is $88\ \Omega$. After modification with HMPDSs, R_{ct} decreased to $35\ \Omega$, revealing that HMPDSs has excellent electrical conductivity. After HMPDSs annealing, R_{ct} value of HMCCSs/GCE is reduced to $8\ \Omega$, demonstrating that HMCCSs has enhanced electrical conductivity to further increase the electron transfer rate on the electrode surface. The EIS results are consistent with the CV data.

To demonstrate the electrocatalytic activity of HMCCSs, the electrochemical behavior of HQ, CC and RS in bare GCE, MPDSs/GCE and in 0.10 M PBS containing 0.1 mM HQ 0.1 mM CC and 0.1 mM RS was investigated via DPV (Fig. 2c). In the case of HMCCSs/GCE, oxidation peaks can be observed for HQ, CC and RS at potentials of -4.1 mV , 104 mV and 440 mV, respectively. The separation of oxidation peak potentials of HQ–CC and CC–RS is about 108.1 mV and 336 mV, respectively. Obviously, HQ, CC and RS can be easily distinguished from one another. Among these electrodes, HMCCSs/GCE has the highest current response for HQ, CC and RS, implying that the HMCCSs composite plays good catalytic effect on electro-oxidation of HQ, CC and RS.

The effective surface area (A_{eff}) of the various working electrode was estimated using Randles-Sevcik equation.

$$I_p = 2.69 \times 10^5 A_{\text{eff}} n^{3/2} D_0^{1/2} \nu^{1/2} C_0$$

where I_p means the anodic peak current (A), A_{eff} is the effective surface area of the different working electrode, n refers to number of electrons participating in the redox reaction, D_0 is diffusion coefficient of 5 mM $[\text{Fe}(\text{CN})_6]^{3-/4-}$ containing 0.1 M KCl ($0.673 \times 10^{-5}\text{ cm}^2\text{ s}^{-1}$), ν is the scan rate (V s^{-1}), C_0 is the concentration of of the redox probe (mol cm^{-3}). The effective surface area of bare GCE, HMPDSs/GCE and HMCCSs/GCE are 0.102 cm^2 , 0.121 cm^2 and 0.135 cm^2 , respectively. The current densities of bare GCE, HMPDSs/GCE and HMCCSs/GCE are calculated to be $212.7\ \mu\text{A}\cdot\text{cm}^{-2}$, $212.4\ \mu\text{A}\cdot\text{cm}^{-2}$ and $209.6\ \mu\text{A}\cdot\text{cm}^{-2}$, respectively.

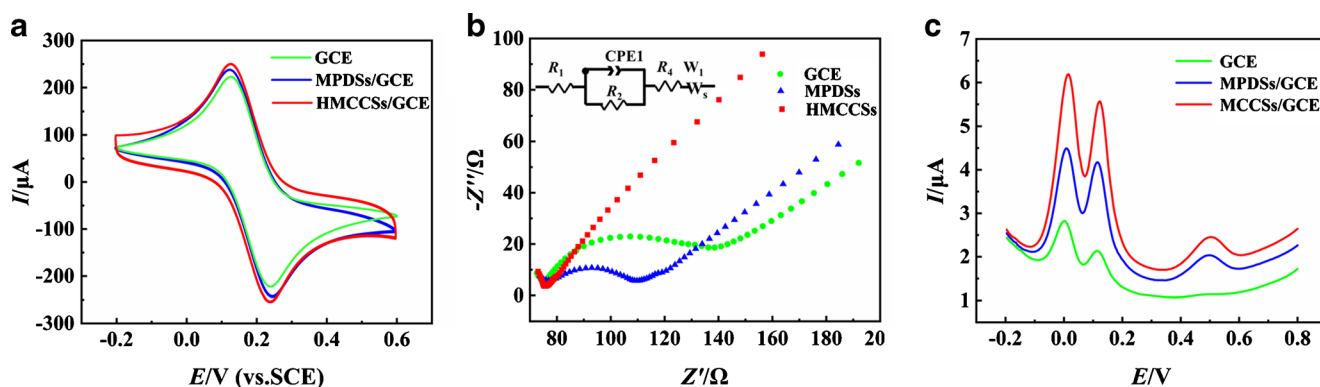


Fig. 2 **a** CV curves and **b** EIS curves of GCE, HMPDSs/GCE and HMCCSs/GCE in 5.0 mM $[\text{Fe}(\text{CN})_6]^{3-/4-}$ containing 0.1 M KCl. The frequency range of EIS was 0.01 Hz~100 kHz. Scan rate was 100 mV s^{-1} .

c Differential pulse voltammetry analysis of different electrodes in 0.1 M PB (pH 7.0) containing 100 μM HQ, 100 μM CC and 100 μM RS

Method optimization

The following parameters were optimized: (a) Sample pH value; (b) scan rate; (c) volume of HMCCSs. Respective data and Figures are given in the Electronic Supporting Material. The following experimental conditions were found to give best results: (a) best sample pH value: 7; (b) the linear relationship between redox peak current and $v^{1/2}$ (30~180 mV s^{-1}) for HQ, CC and RS; (c) best volume of HMCCSs: 5 μL .

Individual determination of HQ, CC and RC in mixed solution

Under the optimal experimental conditions, HMCCSs/GCE was used for individual determination of HQ, or CC, or RS in their mixtures. Figure 3a, c and e shows the individual determination of HQ, or CC, or RS in their mixtures by changing concentration of one component while the other two remaining constant. Figure 3a displays that the oxidation peak current of HQ increased with the increase of the concentration. The peak current response towards HQ increases linearly at the concentration of 0.3~100 μM and 100~1000 μM (Fig. 3b). The similar result is obtained with CC (Fig. 3c) and the two linear ranges (Fig. 3d) are 2~100 μM and 100~2000 μM . Similarly, linear relationships of RS are in the range of 3~80 μM and 80~600 μM (Fig. 3e, f). The detection limit for HQ, CC and RS is calculated to be 0.12 μM , 0.19 μM and 1.1 μM ($S/N=3$), respectively. The sensitivity for HQ, CC and RS is calculated to be 0.75 $\mu\text{A } \mu\text{M}^{-1} \text{cm}^{-2}$, 0.46 $\mu\text{A } \mu\text{M}^{-1} \text{cm}^{-2}$ and 0.074 $\mu\text{A } \mu\text{M}^{-1} \text{cm}^{-2}$ (S/N without cross reaction). And the HMCCSs/GCE sensor has good selectivity and a lower detection limit. The major characteristics of some other electrochemical sensors used for HQ, CC, and RS detection are compared with HMCCSs/GCE (Table 1).

Simultaneous determination of HQ, CC and RC

As shown in Fig. 4, HMCCSs/GCE was used for simultaneous detection of mixed solutions of HQ, CC and RC. When the concentrations of HQ, CC and RC were changed at the same time, the oxidation peak current increased with increasing concentration, whereas their peak potential values remain almost unchanged. The oxidation peak current reveals an outstanding linear relationship with the concentration in the range of 10~250 μM . The detection limit of HQ, CC and RS are 0.045 μM , 0.04 μM and 0.11 μM , respectively ($S/N=3$). The sensitivity for HQ, CC and RS is calculated to be 0.15 $\mu\text{A } \mu\text{M}^{-1} \text{cm}^{-2}$, 0.164 $\mu\text{A } \mu\text{M}^{-1} \text{cm}^{-2}$ and 0.062 $\mu\text{A } \mu\text{M}^{-1} \text{cm}^{-2}$ ($S/N=3$), respectively. It is obvious that the fabricated sensor features a relatively wide linear range and low detection limit.

Reproducibility, repeatability, stability and selectivity

In order to evaluate the reproducibility of the modified electrode, six HMCCSs/GCE were fabricated and used to measure HQ, CC and RS. The relative standard deviations (RSD) are 2.21%, 2.34% and 2.15%, respectively. In addition, the reproducibility of HMCCSs/GCE was investigated by successively measuring the same electrode for five times, and RSD of HQ, CC and RS were 2.21%, 2.34% and 2.15%, respectively. Moreover, HMCCSs/GCE was stored at 4 $^{\circ}\text{C}$ for 14 days and then used for detection of HQ, CC and RS. It was found that the oxidation peak currents of HQ, CC and RS were 95.6%, 94.5% and 95.8% of the initial values. The above results show that the electrode has good reproducibility, repeatability and stability.

To evaluate the selectivity of the electrode, the effects of some co-existing inorganic ions and organic agents were evaluated. It was found that 5 mM Na^+ ,

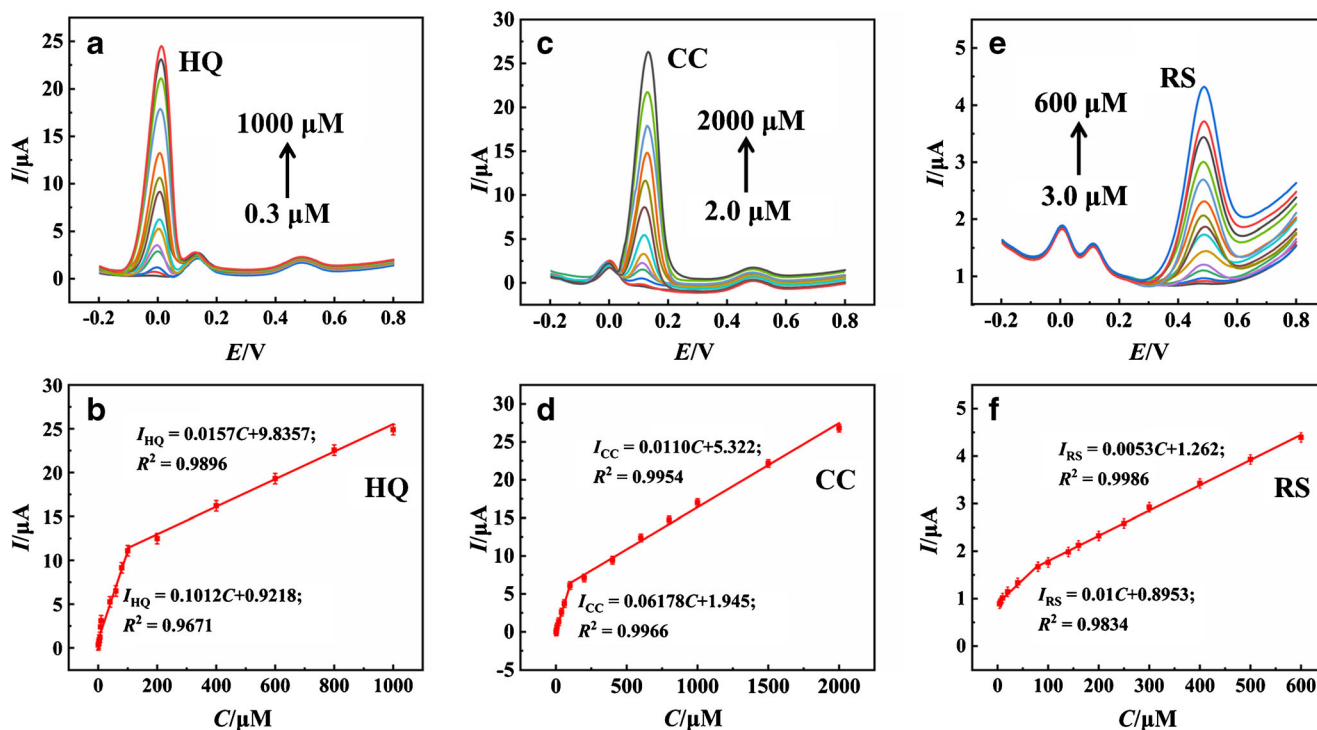


Fig. 3 a DPV curves of HMCCSs/GCE in 0.1 M PB (pH 7.0) containing 20 μM CC, 50 μM RS and different concentrations of HQ (0.3, 4, 6, 8, 10, 40, 60, 80, 100, 200, 400, 600, 800, 1000 μM). c DPV curves of HMCCSs/GCE in 0.1 M PB (pH 7.0) containing 20 μM HQ, 50 μM RS and different concentrations of CC (2, 4, 6, 40, 60, 80, 100, 400, 600, 800,

1000, 1500, 2000 μM). e DPV curves of HMCCSs/GCE in 0.1 M PB (pH 7.0) containing 20 μM HQ, 20 μM CC and different concentrations of RS (3, 6, 10, 20, 40, 80, 100, 140, 160, 200, 250, 300, 400, 500, 600 μM). The corresponding calibration plots between the DPV response and b HQ d CC f RS concentrations ($S/N=3$)

K^+ , Ca^{2+} , Cu^{2+} , Mg^{2+} , Zn^{2+} , Cl^- , NO_3^- , SO_4^{2-} , o-nitrophenol, p-nitrophenol, phenol, ascorbic acid, bisphenol A, humic acids, and glucose had little interference towards the measurements of 50 μM HQ, 50 μM CC and 100 μM RS in 0.1 mM PB (pH 7) (signal change below 5%) (Fig. S6).

Real sample analysis

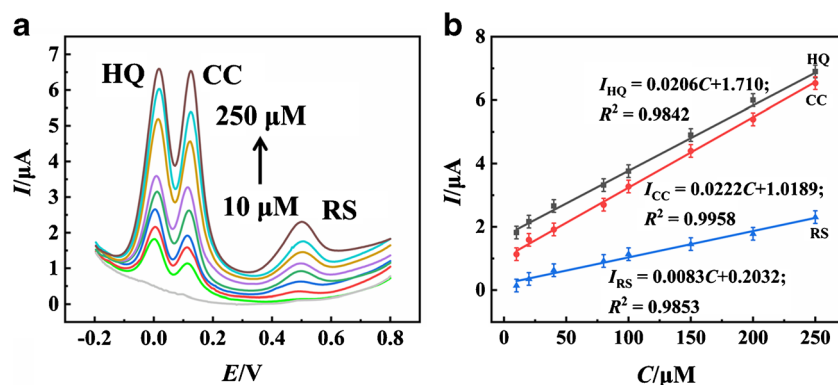
Applicability of HMCCSs/GCE was evaluated by utilizing the developed sensor in detecting tap water, river water and vegetable juice through standard addition method and the results is shown in Table S1. The recoveries of

Table 1 Comparison of HMCCS/GCE with other reported electrochemical sensors in HQ, CC and RS detection. = 3), respectively. The results indicate that the individual determination of HQ, CC and RS in mixed solutions can be tested by this sensor

Electrode	Method	Linear range (μM)			LOD (μM)			Ref.
		HQ	CC	RS	HQ	CC	RS	
Fe/PC ^a /GCE	DPV	0.1~120	1.0~120	–	0.014	0.033	–	[3]
AgNP/MWCNT ^b /GC	SPV	2.5~260	20~260	–	0.16	0.2	–	[5]
Graphene-CS ^c /GCE	DPV	1.0~300	1.0~400	1.0~550	0.75	0.75	0.75	[1]
Ni/N-MWCNT ^d	DPV	0.3~300	0.1~300	–	0.011	0.009	–	[6]
P-Rgo ^e /GCE	DPV	5~90	5~120	5.0~90	0.08	0.18	2.62	[25]
Nitrogen-doped CNT	DPV	10~1000	20~1000	–	1.2	2.71	–	[26]
NMC-G ^f /GCE	DPV	0.5~400	1.0~300	3.0~200	0.15	0.3	1.0	[27]
CDs/r-GO ^g /GCE	DPV	0.5~1000	1.0~950	5.0~600	0.17	0.28	1	[28]
HMCCSs/GCE	DPV	0.3~1000	2.0~2000	3.0~600	0.12	0.19	1.1	This work

^a Fe/PC: porous carbon material doped with an iron species; ^b AgNP/MWCNT: Silver nanoparticles / multiwalled carbon nanotubes; ^c Graphene-CS: graphene-chitosan composite film; ^d Ni/N-MWCNT: Nitrogen-doped multiwalled carbon nanotubes modified with nickel nanoparticles; ^e P-Rgo: porous graphene; ^f NMC-G: nitrogen-doped mesoporous carbon spheres decorated graphene; ^g CDs/r-GO: carbon dots/reduced graphene oxide

Fig. 4 **a** DPV curves of HMCCSs/GCE in 0.1 M PB (pH 7.0) containing different concentrations of HQ, CC and RS (10, 20, 40, 80, 100, 150, 200, 250 μM), **b** calibration graphs for simultaneous determination of HQ, CC and RS ($S/N=3$)



HQ, CC and RS were from 93.5% to 106.5%. In addition, the accuracy of the sensor was confirmed by high performance liquid chromatography (HPLC) (Table S2). By comparison, it was found that there was no significant difference between the two results, indicating that HMCCSs/GCE can accurately analyze the actual sample.

Conclusions

Hollow $\text{Mo}_2\text{C}/\text{C}$ composites was synthesized by a controllable water/ethanol interface reaction, and utilized for the first time to construct electrochemical sensor for simultaneous detection of three dihydroxybenzene isomers. The excellent electrochemical performance of HMCCSs has been confirmed, which is very likely related to their large specific surface area and porous structure. The results indicate that HMCCSs/GCE possessed good electrocatalytic activity. The electrode has been successfully applied to test HQ, CC and RS in real samples with satisfactory recoveries, which fully proves the practicability and reliability of HMCCSs/GCE. The newly developed sensor based on HMCCSs provides a promising platform for environmental monitoring. However, a limitation of the developed sensor is electrode fouling occurring on the macroporous structure of HMCCSs, which may interfere with HQ, CC and RS determination in vivo. Modifying the material and getting super-hydrophobic surface could be one way to alleviate electrode contamination and this will be our future work.

Acknowledgements The project was financially supported by National Natural Science Foundation of China (81773680 and 21575089), free exploration project from the Natural Science Foundation of Shenzhen City (JCYJ20170307150444573) and Scientific Research Foundation for Changjiang Scholars of Shihezi University (CJXZ201501).

Compliance with ethical standards The author(s) declare that they have no competing interests

References

- Yin H, Zhang Q, Zhou Y, Ma Q, Liu T, Zhu L, Ai S (2011) Electrochemical behavior of catechol, resorcinol and hydroquinone at graphene–chitosan composite film modified glassy carbon electrode and their simultaneous determination in water samples. *Electrochim Acta* 56(6):2748–2753
- Jing Z, Ma J, Zhang Y, Lei H, Wan Q (2014) A hydroquinone sensor based on a new nanocrystals modified electrode. *J. Chem. Technol. Biot.* 89 (2):259–264
- Huang, W., Zhang, T., Hu, X., Wang, Y., & Wang, J. (2018). Amperometric determination of hydroquinone and catechol using a glassy carbon electrode modified with a porous carbon material doped with an iron species. *Microchim Acta*, 185(1), 37
- Li, Z., Yue, Y., Hao, Y., Feng, S., & Zhou, X. (2018). A glassy carbon electrode modified with cerium phosphate nanotubes for the simultaneous determination of hydroquinone, catechol and resorcinol. *Microchim Acta*, 185(4), 215
- Goulart LA, Gonçalves R, Correa AA, Pereira EC, Mascaro LH (2018) Synergic effect of silver nanoparticles and carbon nanotubes on the simultaneous voltammetric determination of hydroquinone, catechol, bisphenol a and phenol. *Microchim Acta* 185(1):12
- Rajkumar C, Thirumalraj B, Chen SM, Veerakumar P, Lin KC (2018) Voltammetric determination of catechol and hydroquinone using nitrogen-doped multiwalled carbon nanotubes modified with nickel nanoparticles. *Microchim Acta* 185(8):395
- Naghian E, Najafi M (2018) Carbon paste electrodes modified with SnO_2/CuS , SnO_2/SnS and $\text{Cu}@\text{SnO}_2/\text{SnS}$ nanocomposites as voltammetric sensors for paracetamol and hydroquinone. *Microchim Acta* 185(9):406
- Chao J, Yong L, Wang ZJ, Yue F, Qi W, Yang R (2016) In situ preparation of hollow $\text{Mo}_2\text{C}-\text{C}$ hybrid microspheres as bifunctional electrocatalysts for oxygen reduction and evolution reactions. *J Mater Chem A* 4(32).
- Wan J, Wu J, Xiang G, Li T, Hu Z, Yu H, Liang H, Wan J, Wu J, Xiang G (2017) Structure confined porous Mo_2C for efficient hydrogen evolution. *Adv Funct Mater* 27(45)
- Shon JK, Lee HS, Park GO, Yoon J, Park E, Park GS, Kong SS, Jin M, Choi JM, Chang H (2016) Discovery of abnormal lithium-storage sites in molybdenum dioxide electrodes. *Nat Commun* 7: 11049
- Liu J, Tang S, Lu Y, Cai G, Chen X (2013) Synthesis of Mo_2N Nanolayer coating MoO_2 hollow nanostructures as high-performance anode materials for Lithium-ion batteries. *Energy Environ Sci* 6(9):2691–2697
- Wang Y, Yu L, Lou XW (2016) Synthesis of highly uniform molybdenum-Glycerate spheres and their conversion into

- hierarchical MoS₂ hollow Nanospheres for Lithium-ion batteries. *Angew Chem* 55(26):7423–7426
13. Minakshi SM, Biswal A, Mitchell D, Jones R, Fernandez C (2016) Correlation among physical and electrochemical behaviour of nanostructured electrolytic manganese dioxide from leach liquor and synthetic for aqueous asymmetric capacitor. *Phys Chem Chem Phys* 18(6):4711–4720
 14. Lei L, Wang S, Xiao J, Bian X, Zhang Y, Scanlon MD, Hu X, Yi T, Liu B, Girault HH (2013) A nanoporous molybdenum carbide nanowire as an electrocatalyst for hydrogen evolution reaction. *Energy Environ Sci* 7(1):387–392
 15. Chen WF, Wang CH, Sasaki K, Marinkovic N, Xu W, Muckerman JT, Zhu Y, Adzic RR (2013) Highly active and durable nanostructured molybdenum carbide electrocatalysts for hydrogen production. *Energy Environ Sci* 6(3):943–951
 16. Liu X, Wu D, Ji W, Hou W (2014) Uniform MoO₂@carbon hollow nanospheres with superior lithium-ion storage properties. *J Mater Chem A* 3(3):968–972
 17. Qiu J, Yang Z, Li Q, Li Y, Wu X, Qi C, Qiao Q (2016) Formation of N-doped molybdenum carbide confined in hierarchical and hollow carbon nitride microspheres with enhanced sodium storage properties. *J Mater Chem A* 4(34):13296–13306
 18. Wang Y, Yu L, Lou XW (2016) Formation of triple-shelled molybdenum-Polydopamine hollow spheres and their conversion into MoO₂/carbon composite hollow spheres for Lithium-ion batteries. *Angew Chem Int Ed Eng* 55(47):14668–14672
 19. Shen Q, Zhang X, Li Y, Sun T, Wang C, Qin C (2016) Facile synthesis and electrochemical performances of secondary carbon-coated LiFePO₄-C composite for Li-ion capacitors based on neutral aqueous electrolytes. *J Mater Sci Mater Electron* 27(7):7255–7264
 20. Wang C, Sun L, Zhang F, Wang X, Sun Q, Cheng Y, Wang L (2017) Formation of Mo-Polydopamine hollow spheres and their conversions to MoO₂/C and Mo₂C/C for efficient electrochemical energy storage and catalyst. *Small* 13(32):1701246
 21. Li X, Du X (2017) Molybdenum disulfide nanosheets supported Au-Pd bimetallic nanoparticles for non-enzymatic electrochemical sensing of hydrogen peroxide and glucose. *Sensor. Actuat. B Chem* 239:536–543
 22. Wang M, Shi Y, Zhang Y, Yang W, Huang H, Zhang J, Song J (2017) Sensitive electrochemical detection of bisphenol a using molybdenum disulfide/Au Nanorod composites modified glassy carbon electrode. *Electroanalysis* 29(11):2620–2627
 23. Zeng L, Chen X, Li H, Xiong J, Hu M, Xin L, Li W (2018) Highly dispersed polydopamine-modified Mo₂C/MoO₂ nanoparticles as anode electrocatalyst for microbial fuel cells. *Electrochim Acta* 283: 528–537
 24. Lei Z, Xu L, Jiao Y, Du A, Zhang Y, Zhang H (2018) Strong coupling of MoS₂ Nanosheets and nitrogen-doped graphene for high-performance Pseudocapacitance Lithium storage. *Small* 14(25):e1704410
 25. Zhang W, Zheng J, Lin Z, Zhong L, Shi J, Wei C, Zhang H, Hao A, Hu S (2015) Highly sensitive simultaneous electrochemical determination of hydroquinone, catechol and resorcinol based on carbon dot/reduced graphene oxide composite modified electrodes. *Anal Methods* 7:6089–6094
 26. Zhang H, Bo X, Guo L (2015) Electrochemical preparation of porous graphene and its electrochemical application in the simultaneous determination of hydroquinone, catechol, and resorcinol. *Sensor. Actuat. B Chem* 220:919–926
 27. Amiri M, Ghaffari S, Bezaatpour A, Marken F (2012) Carbon nanoparticle–chitosan composite electrode with anion, cation, and neutral binding sites: Dihydroxybenzene selectivity. *Sensor. Actuat. B* 162(1):194–200
 28. Liu L, Ma Z, Zhu X, Zeng R, Tie S, Nan J (2016) Electrochemical behavior and simultaneous determination of catechol, resorcinol, and hydroquinone using thermally reduced carbon nano-fragment modified glassy carbon electrode. *Anal Methods* 8(3):605–613
- Publisher's note** Springer Nature remains neutral with regard to jurisdictional claims in published maps and institutional affiliations.